SECTION 1

Normal developmental processes

Introduction to Section 1

The advent of magnetic resonance imaging (MRI) in the 1980s and functional MRI in 1991 was revolutionary for developmental clinical neuroscience. In addition to improved resolution relative to older imaging techniques, the lack of ionizing radiation and safety made it ethically possible to study healthy, typically developing children and to do so repeatedly. The rapid development of a variety of techniques, all using conventional MRI scanners, quickly expanded research to allow researchers to study, not only structural brain development, but functional and metabolic development as well.

To provide an understanding of normal brain development, the six chapters in this section describe our current knowledge of and approaches to studying structural and functional brain development. Lu and Sowell describe and richly illustrate the morphological development of the human brain (Chapter 1). Bunge and Crone address the processes, neural correlates of, and developmental changes in, cognitive control (Chapter 2). Gotlib and Joormann discuss emotion regulation and stress reactivity, including both neuroimaging and neuroendocrine aspects (Chapter 3). In Chapter 4, Ernst and Hardin describe a heuristic model of decision making and preliminary developmental findings. In Chapter 5, Pelphrey and Perlman describe key constructs and early findings in the emerging field of developmental social cognitive neuroscience. Finally, McNealy, Dapretto, and Bookheimer provide a comprehensive look at the neural correlates of the multifaceted aspects of language development (Chapter 6).

Not only is the literature described key to understanding healthy, typical, or normal brain development, but it also lays a foundation for understanding deviations in development associated with neuropsychiatric disorders, particularly those beginning in childhood and adolescence. The domains and processes covered are critical to self-regulation and healthy behavioral functioning and are those most often impaired in developmental neuropsychiatric disorders. Much of the work to date has involved cross-sectional comparisons of relatively small samples of different age groups. Going forward, longitudinal designs, increasingly being adopted in structural imaging studies, hold promise for mapping developmental trajectories with improved sensitivity to maturational changes.

1

Morphological development of the brain: what has imaging told us?

Lisa H. Lu and Elizabeth R. Sowell

Introduction

Rapid advances in imaging technology have yielded a significant wealth of knowledge about maturational trajectories of human brain development. Magnetic resonance imaging (MRI) findings are based on signal intensity variations which differentiate tissue types, and regional developmental changes in tissue distribution are thought to reflect cellular changes known from postmortem studies. Imaging studies render longitudinal evaluations possible, and examination of within-subject development across time increases our ability to detect maturational changes embedded within the anatomical variability between individuals. We describe normal morphological maturation findings from three basic approaches for analyzing T_1- and T_2-weighted data: volumetric, voxel-based morphometry (VBM), and cortical pattern-matching (CPM). Researchers are beginning to link morphological changes to cognitive development, and these efforts represent the next wave of fruitful investigations.

Normal morphological maturation

Volumetric image analysis

First attempts to quantify structural maturation in vivo used stereotaxic region definition schemes because image resolution was relatively low (i.e., 4- to 5-mm slice thickness) compared to more recent studies (i.e., 1- to 1.5-mm slice thickness) (Giedd et al., 1996a; Jernigan et al., 1991; Reiss et al., 1996). Some of these studies assessed whole brain tissue volumes (Caviness et al., 1996; Courchesne et al., 2000), while others used manual region definition on a slice-by-slice basis using anatomical landmarks (Giedd et al., 1996b; Lange et al., 1997; Sowell and Jernigan 1998; Sowell et al., 2002c). Algorithms have also been used to warp standardized lobar measures to individual brains and thus define lobar regions automatically (Giedd et al., 1999).

These early studies found decreasing cortical gray matter volume with age while white matter volume increased with age (Jernigan and Tallal, 1990; Jernigan et al., 1991; Pfefferbaum et al., 1994; Reiss et al., 1996) after controlling for differences in overall brain volume (Pfefferbaum et al., 1994; Reiss et al., 1996). Within lobar regions, frontal and parietal lobes increased in gray matter during childhood years (Giedd et al., 1999, 2006; Sowell et al., 2002c) before decreasing during adolescent years (Giedd et al., 1999, 2006). These changes in lobar gray matter volume occurred concomitantly with increasing white matter volume in the corresponding lobes (Giedd et al., 1999, 2006; Sowell et al., 2002c). The most notable changes during childhood and adolescence occurred in more dorsal cortices (Jernigan et al., 1991). More ventral cortices of the temporal lobes changed less dramatically between childhood and

Neuroimaging in Developmental Clinical Neuroscience, eds. Judith M. Rumsey and Monique Ernst. Published by Cambridge University Press.

adolescence (Giedd et al., 1996b; Sowell et al., 2002c). Most studies showed decreasing subcortical gray matter volume with age with overall brain volume controlled (Jernigan et al., 1991; Reiss et al., 1996; Sowell et al., 2002c), although one study found decreasing striatal volume only for boys (Giedd et al., 1996a) and another reported increasing hippocampal volume for girls and increasing amygdalar volume for boys (Giedd et al., 1996b).

Voxel-based morphometry

Volumetric studies can address gross lobar structural changes but are limited in addressing maturational changes with finer spatial resolution. Voxel-based morphometry (VBM) (Ashburner and Friston, 2000), which was initially used to evaluate functional imaging data, has been used to assess structural effects during normal development on a voxel-by-voxel basis (Paus et al., 1999; Sowell et al., 1999a, 1999b). Essentially, VBM entails automated spatial normalization of volumes into a standard coordinate space and scaling of images so that each voxel coordinate is anatomically comparable across subjects. Tissue segmentation and spatial smoothing is then used to assess localized differences in gray matter and/or white matter.

We used VBM to localize age-related gray matter density reductions between childhood and adolescence in 18 normally developing individuals between 7 and 16 years of age (Sowell et al., 1999a). Gray matter density refers to the proportion of signal intensity that is segmented as gray matter by automated segmentation software within a smoothing kernel. We found that gray matter volume reduction observed in frontal and parietal lobes in the volumetric studies was mainly driven by gray matter density reduction in the dorsal region of these cortices. The parietal cortex changed the most in both the volumetric and VBM assessments of gray matter, and relatively little change occurred in the more ventral cortices of the temporal and occipital lobes (Figure 1.1). The prominent finding in the parietal lobes, relative to the frontal lobes, was not expected given the known posterior to anterior progression of maturational cellular events. We tested the hypothesis that frontal lobe changes occur later in adolescence by conducting a VBM study focusing on the adolescent to adult age range (Sowell et al., 1999b). Whereas cortical changes were

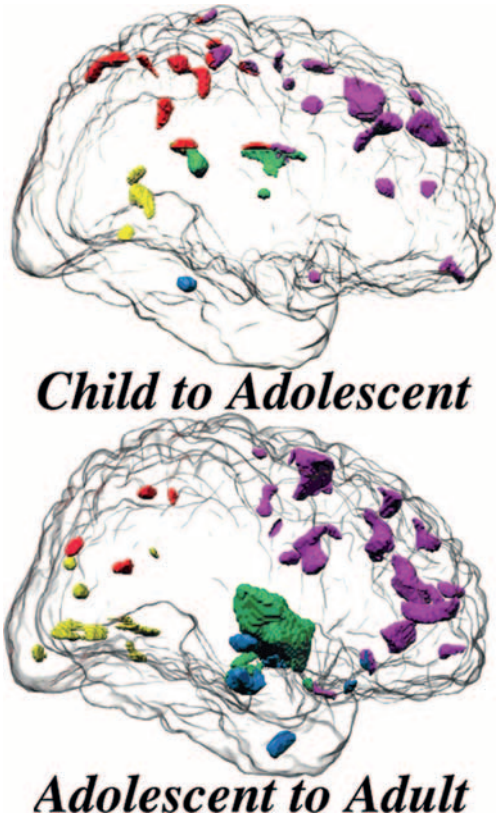

Figure 1.1. Age-related reductions in gray matter density. *Top*: Statistical map representing gray matter density reduction between childhood and adolescence. *Bottom*: Gray matter density reduction between adolescence and adulthood. These maps are three-dimensional renderings of traditional statistical maps shown inside the transparent cortical surface of one representative subject's brain. Lobes and the subcortical region were defined anatomically on the same subject's brain. Color coding is applied to each cluster based on its location within the representative brain. Clusters are shown in the frontal lobes (*purple*), parietal lobes (*red*), occipital lobes (*yellow*), temporal lobes (*blue*), and subcortical region (*green*). Reproduced with permission from Sowell et al. (2004b).

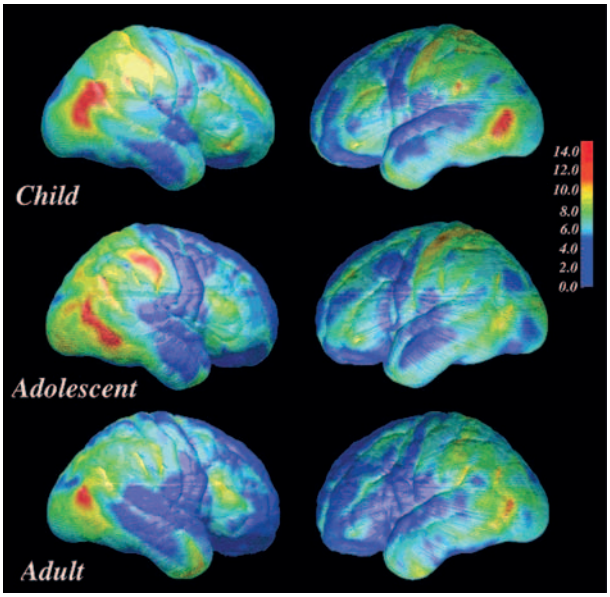

Figure 1.2. Age-related differences in cortical surface variability. Maps showing cortical surface variability in the average child ($n = 14$), the average adolescent ($n = 11$), and the average young adult ($n = 10$). The color bar indicates variability within each group as the root mean square magnitude (in mm) of displacement vectors required to map each individual onto the group average surface mesh. Note that this map is representative of residual brain shape variability after affine transformation (translation, rotation, scaling, and skew/shear) into the standard space created by the International Consortium for Brain Mapping from 305 normal adult brains. Higher variability is observed in posterior temporal regions and in the postcentral gyrus in all three age groups, with relatively less variability in precentral and anterior temporal gyri. Adapted with permission from Sowell et al. (2002b).

diffusely distributed in dorsal frontal and parietal regions between childhood and adolescence, cortical maturation between adolescence and adulthood was localized to large regions of dorsal, mesial, and orbital frontal cortex with relatively little gray matter density reduction in other brain regions (Sowell et al., 1999b), as shown in Figure 1.1. These results are consistent with studies showing that the frontal lobes are essential for such functions as response inhibition, emotion regulation, planning, and organization (Fuster, 2001), which may not be fully developed in adolescents.

Figure 1.1 also shows gray matter density reductions in subcortical structures. Gray matter density loss in the lentiform nuclei was more evident between adolescence and adulthood (Sowell et al., 1999b). In a study that examined white matter change using VBM, Paus and colleagues found prominent white matter density increases in the arcuate fasciculus in the temporo-parietal region and in the posterior limb of the internal capsule in subjects 4–17 years of age (Paus et al., 1999).

Cortical pattern-matching

A limitation with VBM is that brain volumes are typically spatially normalized across subjects using automated image registration. Current VBM techniques cannot control for variability in sulcal patterns across individuals. Variability in sulcal patterns differs by cortical region and is more pronounced the further the region is from the center of the brain. As shown in Figure 1.2, sulcal pattern can vary up to 14 mm even after spatial normalization, particularly in the

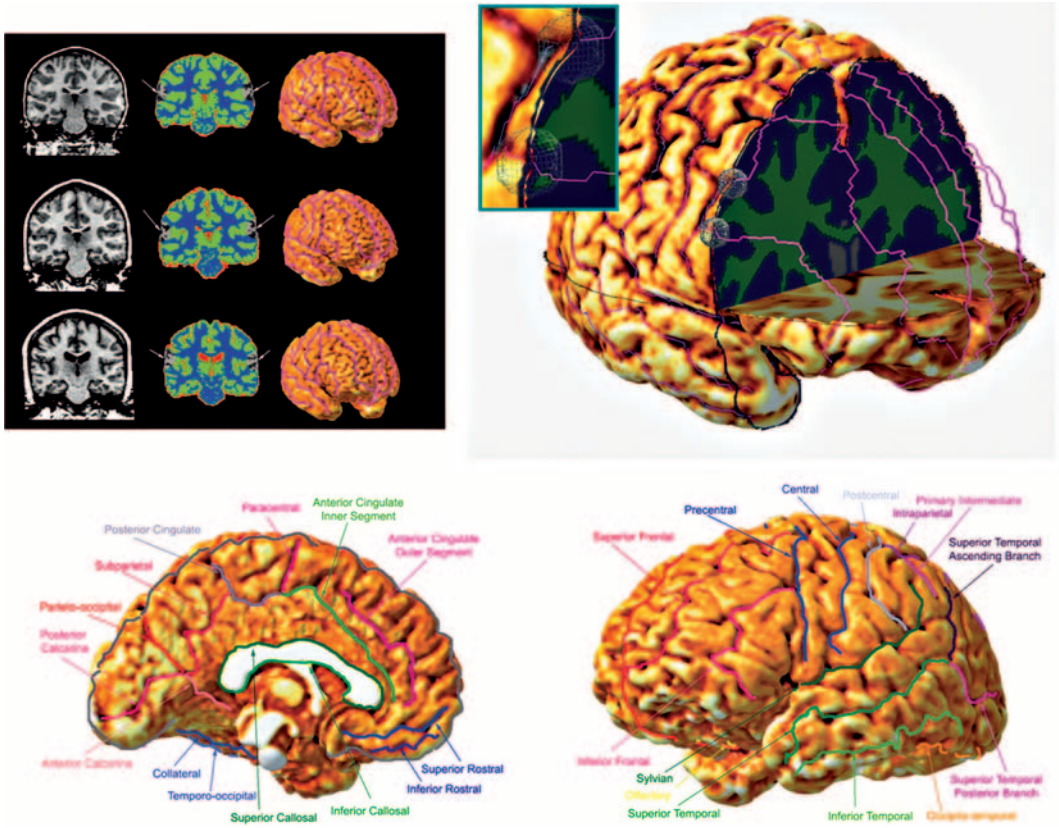

Figure 1.3. Cortical pattern-matching (CPM) methods. *Top left*: Three representative brain image data sets with the original MRI, tissue-segmented images, and surface renderings, with sulcal contours shown in pink. *Top right*: Surface rendering of one representative subject with cutout showing tissue-segmented coronal slice and axial slice superimposed within the surface. Sulcal lines are shown where they would lie on the surface in the cutout region. Note the sample spheres over the right hemisphere inferior frontal sulcus (lower sphere) and on the middle region of the precentral sulcus (upper sphere) that illustrate varying degrees of gray matter density (GMD). In the blown-up panel, note that the upper sphere has a higher GMD than does the lower sphere as it contains only blue pixels (gray matter) within the brain. The lower sphere also contains green pixels (white matter) that would lower the GMD within it. In the actual analysis, GMD was measured within 15-mm spheres centered across every point over the cortical surface. *Bottom*: Sucal anatomical delineations are defined according to color. These are the contours drawn on each individual's surface rendering according to a reliable, written protocol (Sowell et al., 2002b). Reproduced with permission from Sowell et al. (2004b).

posterior temporal regions (Sowell et al., 2002b). Without taking this variability into account, VBM techniques are not likely to match cortical surface regions well across subjects. Cortical pattern-matching (CPM) methods (Thompson et al., 2004) allow us to account for interindividual differences in cortical patterns and achieve better matching of cortical anatomy across subjects, which may improve statistical power to localize age-related changes. Figure 1.3 depicts some major steps involved in using CPM methods. Briefly, CPM involves creating a three-dimensional geometric model of the cortical surface extracted from the MRI volume (MacDonald et al., 1994) and then flattening it to a

two-dimensional planar format (Thompson and Toga, 1997; Thompson and Toga, 2002). A warping transformation is then applied that aligns the sulcal anatomy of each subject with an average sulcal pattern derived for the group. To improve sulcal alignment across subjects, all sulci that occur consistently can be manually defined on the surface rendering and used as anchors to restrict this transformation. Once cortical pattern and shape have been matched across subjects, morphological measures such as gray matter thickness or distance of the surface from the center of the brain (reflecting localized brain growth) can then be compared with greater anatomical accuracy. This method of measuring gray matter thickness has been validated against histological data (Sowell et al., 2004a). We have measured both gray matter thickness (i.e., distance from the white matter/gray matter interface to the gray matter/cerebrospinal fluid border) and gray matter density. Because both methods of quantifying gray matter yield very similar results, we will use the term gray matter density (GMD) for the remainder of the chapter. Cortical pattern-matching techniques can also be used to study cortical expansion, brain surface asymmetry, and subcortical growth. Combined, these studies have highlighted regional patterns of cortical change with age that have not been appreciated with techniques such as volumetric image analysis or VBM.

Gray matter density

Gray matter density studies using CPM have largely concurred with findings from VBM studies. In a study of 35 individuals between 7 and 30 years of age, we found local GMD loss distributed over the dorsal frontal and parietal lobes between childhood and adolescence (Sowell et al., 2001b). Between adolescence and adulthood, a dramatic increase in local GMD loss was observed in the frontal lobes, parietal GMD loss was reduced relative to earlier years, and a relatively small, circumscribed region of local GMD increase was observed in the left peri-Sylvian region. We tested for non-linear age effects on GMD change in a larger sample of 176 normal individuals ranging in age from 7 to 87 years (Sowell et al., 2003). As shown in Figure 1.4, non-linear age effects were significant over most dorsal aspects of frontal and parietal regions and in the orbitofrontal cortex. There was a dramatic decline in GMD between 7 and 60 years of age. This pattern in attenuated form was evident in most lateral and medial brain surface regions (Figure 1.5) except for the peri-Sylvian region in the inferior parietal and posterior temporal cortices (Figure 1.4). The non-linear age effects in bilateral peri-Sylvian regions were inverted, showing a subtle increase in GMD in the first three decades of life, then a decline in later decades (Figure 1.4).

We were able to corroborate cortical thickening in the peri-Sylvian region using a separate longitudinal data set of children between 5 and 11 years of age (Sowell et al., 2004a). Again, bilateral peri-Sylvian thickening was found, but in the left hemisphere, thickening was extended more anteriorly to encompass the inferior frontal gyrus. In contrast, Gogtay and colleagues did not find increasing GMD in the peri-Sylvian region of 13 subjects (age ranged from 4 to 21 years) studied longitudinally (Gogtay et al., 2004). They found a flat GMD growth curve in superior temporal gyrus and inferior frontal gyrus. However, this growth pattern did contrast with the growth pattern in remaining regions of the brain, where GMD loss was seen, similar to our findings. These findings from different data sets across independent research groups corroborate that the growth pattern of the peri-Sylvian region differs from that of remaining regions of the cortex. Gogtay and colleagues also corroborate the pattern of GMD loss we observed between childhood and adulthood (Sowell et al., 2001b). They found evidence of GMD loss in dorsal parietal cortices early in development, then spreading rostrally over the frontal cortex and caudally and laterally over the parietal, occipital, and temporal cortices during adolescence (Gogtay et al., 2004). Within frontal and parietal subregions, GMD loss progressed from primary cortices (precentral and postcentral gyri) to association and tertiary cortices. Frontal, occipital, and temporal poles matured early, whereas

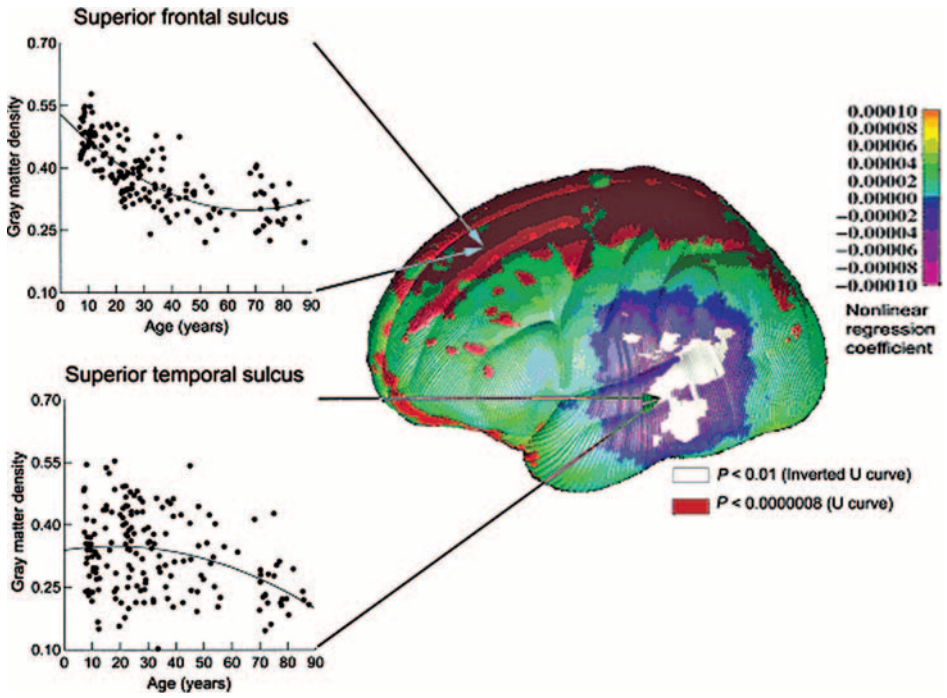

Figure 1.4. Statistical map of nonlinear age effects of gray matter density (GMD) on the lateral brain surface. This left frontal view shows age effects of GMD on the lateral surface of the brain between childhood and old age. Regions shown in red correspond to regression coefficients that have statistically significant positive non-linear age effects at a threshold of $p = 0.000\,000\,8$ (U-shaped curves with respect to age), and regions shown in white correspond to statistically significant negative non-linear age effects at a threshold of $p = 0.01$ (inverted U-shaped curves). Shades of green to yellow represent positive partial regression coefficients for the quadratic term, and shades of blue, purple and pink represent negative partial coefficients. The pattern of non-linear age effects was similar in the left and right (not shown) hemispheres, except that none of the negative non-linear age effects in the right posterior temporal lobe reached a threshold of $p = 0.01$. Scatterplots of age effects with the best-fitting quadratic regression curve are shown for sample surface points in the superior frontal sulcus (top) and the superior temporal sulcus (bottom). Gray matter density within the 15-mm sphere centered on the sample surface point (matched across subjects) is shown on the *y*-axis. Reproduced with permission from Sowell et al. (2003).

other parts of the temporal lobe matured last (Gogtay et al., 2004).

Cortical expansion

The precise relationship between signal change as detected on MR images and actual physiological changes taking place at the cellular level is not yet clear. It is known from postmortem studies that synaptic pruning and loss of dendritic processes occur during childhood and adolescence, with synaptic elimination ending earlier in primary sensory cortices (around age 12) than in the prefrontal cortex (around age 16) (Huttenlocher, 1979; Huttenlocher and Dabholkar, 1997; Huttenlocher and De Courten, 1987). Increase in GMD may be affected by the number, size, and packing density of neurons, which, in turn, are affected by genetics, hormones, growth factors, nutrients, and other environmental variables (e.g., toxins, trauma, stress,

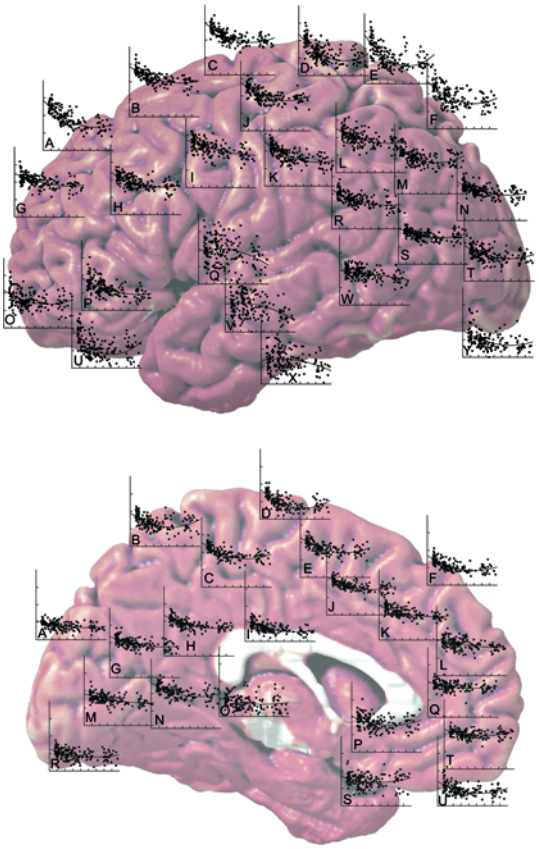

Figure 1.5. Scatterplots of gray matter density (GMD) on lateral (top) and medial (bottom) left hemisphere surfaces. Shown are scatterplots for GMD at various points over the brain surface where measurements were taken. The axes for every graph are identical to those in Figure 1.4. Age in years is represented on the *x*-axis (range 0–90) and GMD on the *y*-axis (range 0.1–0.7). *Top*: Anatomical location associated with each graph on the lateral surface: (A) superior frontal gyrus, (B) superior frontal sulcus (SFS), middle region, (C) SFS, posterior region, (D) precentral gyrus, (E) postcentral gyrus, (F) superior parietal gyrus, (G) SFS, anterior region, (H) inferior frontal sulcus (IFS), middle region, (I) IFS, posterior region, (J) precentral sulcus, (K) central sulcus, (L) postcentral sulcus, (M) intraparietal sulcus, (N) secondary intermediate sulcus, (O) olfactory gyrus, (P) IFS, anterior region, (Q) Sylvian fissure, (R) primary intermediate sulcus, (S) superior temporal sulcus (STS), ascending branch, (T) transverse occipital sulcus, (U) olfactory sulcus, (V) STS, main body, (W) STS, posterior branch, (X) inferior temporal sulcus, (Y) inferior occipital gyrus. *Bottom*: Anatomical location associated with each graph on the medial surface: (A) cuneus, (B) pre-cuneus, (C) posterior cingulate, (D) precentral gyrus, (E) paracentral sulcus, (F) superior frontal gyrus, (G) parieto-occipital sulcus, (H) subparietal sulcus, (I) isthmus region, (J, K, L and Q) anterior cingulate, (M) posterior calcarine sulcus, (N) anterior calcarine sulcus, (O) callosal sulcus, (P) genu, (R) retrocalcarine sulcus, (S) gyrus rectus, (T) superior rostral sulcus, (U) frontomarginal gyrus. Adapted with permission from Sowell et al. (2003).

enrichment level of the environment) (Giedd et al., 1996a). Concomitant with these neuronal changes is the proliferation of myelination, which begins near the end of the second trimester of fetal development and is protracted into the second decade of life and beyond (Yakovlev and Lecours, 1967). Giedd and colleagues have hypothesized that myelination is primarily responsible for changes in the size of the brain and its components, as it is estimated that a total loss of synaptic boutons would account for only a 1%–2% decrease in volume (Giedd et al., 1996a).

Examining localized brain growth together with changes in GMD may provide clues regarding cellular mechanisms underlying GMD change. Some have speculated that cortical thinning could in part be due to increased proliferation of myelin into the periphery of the cortical neuropil. In other words, tissue with gray matter signal in the younger subjects may actually be unmyelinated peripheral fibers, so the MR signal value that is "gray matter" in the younger subjects could change to white matter in the older subjects (for a discussion see Sowell et al., 2003, 2004b). Data from our laboratory and others using volumetric methods suggest that gray matter is replaced by white, given that white matter volumes increase and gray matter volumes decline (Courchesne et al., 2000; Giedd et al., 1999; Jernigan et al., 1991). Our CPM studies of localized brain growth described below suggest that "gray matter" thinning may not be the best term to

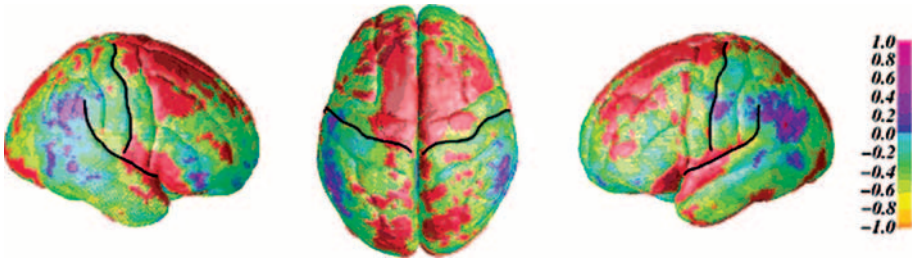

Figure 1.6. Statistical map of the correlation between gray matter density (GMD) and distance from center (DFC) across 35 individuals from 7 to 30 years of age. Anatomically, the central sulcus and Sylvian fissure are highlighted. Highlighted in red are regions where the negative relationship (i.e., less GMD associated with more extensive DFC) is highly statistically significant ($p = 0.000\,001$). Shown in shades of green to yellow are regions where the negative correlation between GMD and DFC does not reach threshold of $p = 0.05$. Shown in shades of blue, purple, and pink are regions where the correlation is positive. Note that none of the positive correlations between GMD and DFC is significant, even when $p = 0.01$ was used as a threshold. © 2001 by the Society for Neuroscience Sowell et al. (2001b).

describe morphological changes we observe with MRI (Sowell et al., 2001b, 2004a).

We quantified localized brain growth by measuring the distance from the midline decussation of the anterior commissure ($x = 0$, $y = 0$, $z = 0$) to each of the 65 536 matched brain surface points. Differences in the length of the distance from center (DFC) line at each brain surface point between different age groups (e.g., children and adolescents) suggest local growth in that location, and statistical analysis at each point can be conducted. In a group of 35 individuals between 7 and 30 years of age, we found brain growth in bilateral dorsal frontal and parietal regions that correlated significantly with concomitant GMD loss (Figure 1.6) (Sowell et al., 2001b). In these regions, thinner gray matter was associated with more brain expansion. Myelination would presumably only result in volume increase, given that myelin consists of space-occupying glial cells (Friede, 1989), whereas neuronal factors underlying maturation could be associated with either volume decrease (due to synaptic pruning) or volume increase (increase in soma size, expansion of dendritic arborization, etc.). Gray matter density loss simultaneous with brain expansion in the dorsal frontal and parietal regions likely resulted from a combination of increased myelination and neuronal factors, as it is known that expansion of myelin into the cortical neuropil could result in a reduction of brain tissue that segments as gray matter on MRI, and non-myelinated fibers do not have typical white matter value signals on T1-weighted images (Barkovich et al., 1988). Interestingly, GMD gain in the inferior parietal regions did not correlate significantly with localized brain expansion, nor did brain expansion in the temporo-occipital junction correlate with GMD gain (Sowell et al., 2001b).

Brain surface asymmetry

Asymmetries in sulcal patterns are of considerable interest, particularly in the peri-Sylvian region given the functional lateralization of language in this region (reviewed in Geschwind and Galaburda, 1985). Postmortem studies have shown that, in adults, the Sylvian fissure is longer in the left hemisphere compared to the right (Galaburda et al., 1978; Ide et al., 1996), and in vivo vascular imaging studies have shown that the Sylvian fissure angles up more dramatically at its posterior end in the right hemisphere compared to the left (LeMay and Culebras, 1972). Greater left planum temporale length in the left hemisphere compared to the right has been observed in postmortem studies of infants, indicating that these asymmetry patterns may be independent of maturational change and